

TRUE-LOSSLESS AUTOENCODER RESIDUAL COMPRESSION (TLARC) FOR HIGH-RESOLUTION SATELLITE IMAGERY

Prithviraj^{1*}, Rajesh I. S.², Bharathi Malakreddy A.³

¹BMS Institute of Technology and Management, Bengaluru, Affiliated to Visvesvaraya Technological University, Belagavi, Karnataka, India, prithvijain28@gmail.com

²Department of AI and ML, BMS Institute of Technology and Management, Bengaluru, Affiliated to Visvesvaraya Technological University, Belagavi, Karnataka, India, is.rajesh081@gmail.com

³Department of AI and ML, BMS Institute of Technology and Management, Bengaluru, Affiliated to Visvesvaraya Technological University, Belagavi, Karnataka, India, bharathi_m@bmsit.in

Corresponding Author: Prithviraj (Email: prithvijain28@gmail.com)

Abstract: The high rate of proliferation of earth observation missions has resulted in the production of very large quantities of high-resolution satellite imagery with on-board processing posing serious challenges because of storage capacity, bandwidth, and real time transmission expense. The classical lossless and near-lossless compression methods are based on predetermined transformations, including DCT, DWT, or predictive entropy coding, that are typically not capable of deriving the spatial-spectral correlation and structural variations in satellite data. To overcome such drawbacks, we introduce a True-Lossless Autoencoder Residual Compression (TLARC) model consisting of a convolutional autoencoder plus deterministic residual compression in order to provide a model with a perfect pixel-level reconstruction and high compression efficiency. The encoder is trained on a small data-driven latent representation that can be on different land-cover types, cloud coverage, and illumination levels. A quantization module encodes Latent activation values into values that can be stored as integers, and the values corresponding to the quantization differences, which are usually discarded in the standard autoencoder approaches, are encoded as tensors of the residual values. These tensors are reintroduced back after decoding to obtain perfect reversibility and actual lossless reconstruction. Largely-scale experiments have shown that TLARC has always been offering an ideal fidelity, lower storage and better compression. The proposed method has a compression ratio of 2.18x \pm 0.08, bit rate of 10.98 bpp, and space savings of over 54% and the encoding and decoding time are 0.182 s and 0.157 s respectively. These results affirm the fact that TLARC is better than the conventional compression techniques..

Keywords: Satellite Image Compression, True-Lossless Reconstruction, Convolutional Autoencoder, Residual Preservation, Quantization Error Recovery.

1. INTRODUCTION

Imaging as a form of information perception and communication has become an essential part of almost all areas of modern science and technology. Images do not only provide visual information in an intuitive way but also maintain detailed spatial and contextual correlations that plays important role in both qualitative and quantitative analysis. The era of digital transformation has seen imaging systems being ubiquitous, starting with consumer electronics to sophisticated scientific instrumentation. The unending development of imaging sensors, especially those installed in remote sensing satellites has resulted in an enormous increase in the creation of high-resolution images [1]. The increase in sensor resolutions and expansion in spectral sensitivity has led to increased data volumes which

have increased exponentially resulting in a big challenge in data storage, transmission and effective organization of the image data [2].

Modern satellite technologies have enabled Earth observation (EO) systems to obtain information in extremely broad spatial, spectral, and temporal resolution [3]. The satellite imagery made available by satellites like Landsat, SPOT, Sentinel and WorldView are available at spatial resolutions as small as sub-meters, and with tens or hundreds of spectral bands in multispectral and hyperspectral sensors [4]. These systems are complemented by CubeSats and microsatellite constellation, which comes in with high temporal revisit frequencies. Such imaging capabilities lead to the continuous data stream, and sometimes, a single mission can receive several terabytes of information per day. The total amount of data stored each year can easily go to petabytes when aggregated among various sensors, missions, and ground stations. As a result, effective data compression has become a mandatory requirement of end-to-end remote sensing data pipelines that include onboard storage, downlink transmission, ground processing, and long-term archiving. [5] Thus, efficient data compression has become absolute necessity for these types of end-to-end remote sensing data pipelines encompassing onboard storage, downlink transmission, processing and archiving.

The image compression approaches mainly focus on reduction of amount of data required to present an image appropriately while maintaining the acceptable visual and analytical quality. Generally, the traditional approaches of image compression are categorized as lossless and lossy methods [6]. The reconstruction performed by lossless images is identical to the original image and it preserves every attribute of original image during reconstruction because these features play important role for scientific or analytical tasks. This characteristics of feature preservation plays important role in different applications such as environmental monitoring, change detection, mineral mapping and many more where minor distortion and poor data quality can lead to incorrect interpretations. However, these methods achieve relatively modest compression ratios. On the other hand, the lossy compression schemes are also widely adopted in various applications where bandwidth saving is the priority. The lossy compression techniques yield much higher compression rate by discarding the visually or statistically redundant information. The visually or statistically redundant information that has little analytical significance. However, this approach helps to enhance the transmission and storage efficiency but it may also introduce distortions or spectral artifacts which can limit their utilization in tasks demanding radiometric precision.

Traditionally, JPEG, JPEG2000 and SPIHT are widely adopted compression techniques [7]. These techniques mainly use the transformation-based decorrelation, quantization and entropy coding in order to take advantage of spatial redundancy existing in images. JPEG utilizes the discrete cosine transforms over non-overlapping blocks whereas JPEG2000 takes advantage of it by using a discrete wavelet transform (DWT) that captures multiscale dependencies [8]. SPIHT (Set Partitioning in Hierarchical Trees) is a progressive bit stream coder that has scalable performance when using different bit rates [9]. Although these approaches are successful in natural images, they are not applicable to satellite images because of a number of peculiarities. Satellite imagery tend to be very spatially variable, highly correlated in spectral between neighboring bands, and have non-uniform distributions of noise due to atmospheric and sensor effects. Moreover, the dissimilarities in sensor design, orbit and light conditions result in non-uniform distributions that cannot be generalized well by handcrafted coding schemes.

In satellite image scenarios, the Inter-band dependencies are strong in the case of hyperspectral imagery thus compression becomes a tedious task. Currently there are three-dimensional transforms, including 3D-DCT or 3D-DWT [10], or correlation-based learning based on principal component analysis (PCA), independent component analysis (ICA), and prediction-based methods which are used to combine spatial and spectral redundancies. The operational cost of such methods is higher thus limiting their operational use, particularly on limited platforms such as satellites. Furthermore, transform coding does not cope with local texture and edges, so any smooth variations in a stream are well-conserved but when compression ratio is high, then the block becomes visible, thus deteriorating.

Other than transform coding, many model based and predictive coding algorithms have been suggested to enhance compression performance. Differential pulse code modulation (DPCM), context-based adaptive lossless image coding (CALIC) and adaptive linear prediction are some of the predictive techniques that have demonstrated potential in lossless and near-lossless compression schemes [11]. These methods take advantage of the fact that there exist correlations between neighbouring pixels or bands and approximate the pixel value and just encode the residuals. However, their effectiveness depends upon the effective modeling of image statistics which are more complicated in multisensor and multitemporal data. Over the past few years, the popularization of deep learning structures has transformed the field of image compression. In contrast to traditional hand-crafted codecs, deep learning models are trained to automatically learn hierarchical feature representations that have the ability to effectively model complex data distributions. Convolutional neural networks (CNNs), autoencoders and variational autoencoders (VAEs) [12],

and generative adversarial networks (GANs) [13] have shown that small, latent representations can represent both local spatial features and global scene semantics.

In the case of satellite imagery, compression using deep learning has several benefits. First, it has the capability to model non-linear spatial and spectral dependencies in a wide range of imaging modalities without explicit feature engineering. Second, these models are trained with huge amounts of data of various satellites and states, which allows them to be generalized to new scenes. Third, these methods can work in hybrid configurations, with support of lossy and lossless compression with learned quantization and entropy modeling layers. Further, the neural compression models can be optimized to address the downstream tasks in classification, segmentation, anomaly detection, and change detection. This makes it possible to optimize not only the perceptual quality, but the task-relevant performance in which the encoding is determined by the preservation of semantically significant information.

An encoder-decoder scheme is a common compression scheme based on deep learning. The encoder is used to convert the input image into a lower-dimensional representation in latent space, typically hierarchically abstracted via convolutional or attention-based layers. This latent code is quantized and entropy-coded. The decoder does the reverse process and restores the original image [14]. However, there are still obstacles to implementing the use of deep neural compression techniques in the deployment of satellite systems that are in operation. The complexity of the models and the needs of computations are high and this makes it challenging to implement them on boards. Satellites have power limitations, radiation tolerance, and limited memory that limit the viability of big networks. Furthermore, the need to support close real-time functionality in data capture as well as transmission requires lean architectures and effective quantization schemes.

To overcome the issues of traditional methods, we present a deep learning-based approach for satellite image compression. The proposed approach leverages the representational power of CNN and residual based coding. The complete approach combines autoencoder based feature extraction, Quantization and Latent Encoding, and lossless reconstruction.

The rest of the article is organized as follows: section II presents brief literature review about existing compression methods, section III presents the detailed discussion about proposed model, section IV presents the outcome of proposed model and finally section V presents the concluding remarks.

2. LITERATURE REVIEW

As the spatial, spectral and temporal resolution of modern satellites is increasing too fast, the efficient compression of remotely sensed imagery has emerged as a key demand in storage, transmission and on-board processing. JPEG2000 and the CCSDS recommendations are some of the most commonly used traditional image compression standards however, these methods fail to achieve high compression ratio and reconstruction quality. Moreover, these systems face challenges particularly when dealing with hyperspectral or multispectral data with complicated textures and fine spatial detail. These traditional methods are increasingly challenged by the increasing data acquisition rates to achieve a balance between the fidelity, compression efficiency and the computational complexity in resource-constrained satellite environments.

In order to mitigate these issues, recent studies have considered deep learning-based compression models, which are capable of end-to-end learning to compress and denoise satellite images without manually selecting parameters, or being aware of noise dynamics. de Oliveira et al. [15] investigated a convolutional neural network (CNN) based compression and denoising of satellite imagery, which can learn to reduce the area taken by the image and remove noise without the need for human-tuning of parameters. This work proposed a modular architecture and onboard joint compression-denoising framework, which executes onboard compression before ground-based denoising, hence providing the flexibility in the computational distribution and showing the possibility of performing neural compression directly on satellites.

Xiang et al. [16] proposed HL-RSCompNet, a deep compression network specifically designed to work with remote sensing images, and applies discrete wavelet transformation (DWT) to separate the features into high- and low-frequency features. Their technique, which simultaneously encodes these frequency components using a separate frequency-domain encoder-decoder, retains more high-frequency detail and improves the fidelity of reconstruction than more traditional methods. Zhao et al. [17] developed compression fidelity further by using an adversarial learning framework, a Symmetrical Lattice Generative Adversarial Network (SLGAN) with symmetric encoder-decoder lattices and cooperating discriminators. Addition of an Enhanced Laplacian of Gaussian (ELoG) loss enabled better reconstruction of edges, contours and textures in reconstructed images.

Similarly, in another study, Cheng et al. [18] used conditional GANs to compress remote sensing images, with adversarial learning improving fine details and realism of the texture. To alleviate one of the fundamental weaknesses of CNN-based models in texture restoration, this model integrated a Laplacian of Gaussian loss and perceptual metrics to enforce visually consistent reconstruction. Similarly, Xiang et al. [19] proposed LRCompNet, a light long-range convolutional compression network, which can capture the large spatial dependency with a non-local attention mechanism to enhance the compression quality and minimise the computation expenses. Applying this concept to multispectral data, Kong et al. [20] introduced MSSSA-Net, a multi-scale spatial-spectral attention network that is based on a variational autoencoder (VAE) architecture. This model is able to capture non-stationary spectral correlations and multi-scale spatial features at the same time with greater adaptability to a variety of remote sensing scenes.

Joshi et al. [21] introduced a lossless compression algorithm of onboard hyperspectral data that relies on spatial and spectral correlation by using non-binary tree traversal (NBTT) and neighbor-driven decision-making (NDDM). This method minimizes prediction errors and computation and it is applicable to real-time onboard applications. Gu et al. [22] developed a lossless compression model which uses lossy-compressed priors via Lossy Prior Probability Prediction Network (LP3Net). The method used checkerboard segmentation, lossy sub-image compression, and probability-based prediction which enabled the method to perform better under lossless performance without compromising efficiency. Giuliano et al. [23] studied variational autoencoders (VAEs) as a method to compose but also to use them in downstream tasks of machine learning, such as classification. Their work showed that the latent representations recovered at compression could be directly used in classifiers without reconstructing the images, a new direction in task-aware compression which can at once facilitate the reduction of storage and onboard inference. Abramova et al. [24] aimed at enhancing the performance of DCT-based lossy compression, suggesting a fast and precise prediction of the mean square error (MSE) of compressed images under local activity analysis, without the need of any parameter tuning and providing the opportunity of adaptive control of the quality. Recent research works in compression field have shown significant improvements and paved the way for future research works [25-27].

3. PROPOSED MODEL

This section presents the detailed discussion about proposed approach where deep learning concept has been utilized to present a lossless compression scheme for satellite images. the proposed model combines the convolutional autoencoder module with a residual correction mechanism to achieve the perfect reconstruction of compressed image. The overall design focus on combining the representational efficiency of neural networks and the deterministic reversibility needed by lossless compression.

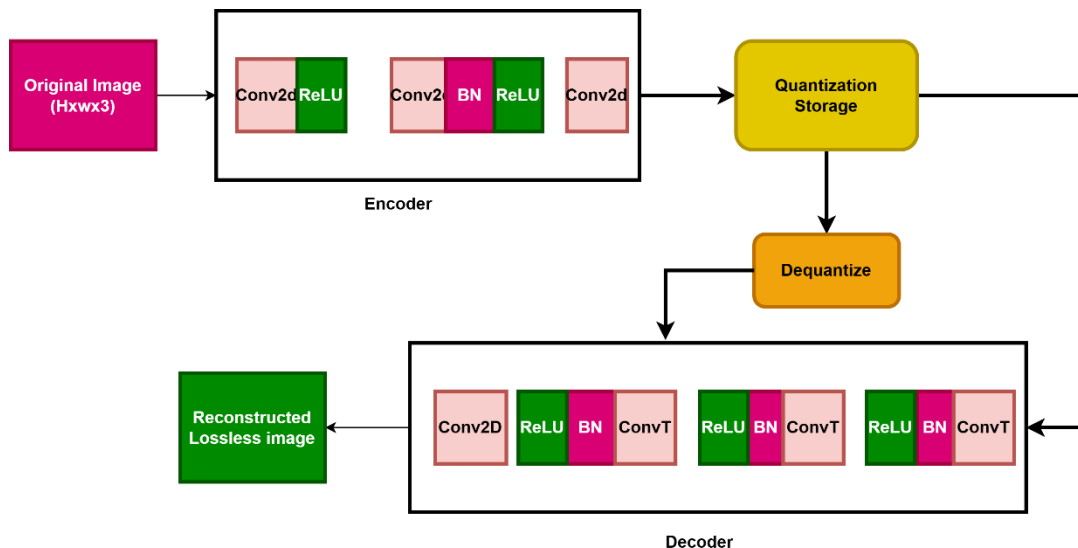


Fig. 1 Overall architecture of proposed model

Overview

As discussed, the satellite imagery generated by modern earth observation system poses severe challenges in terms of storage, transmission and real-time processing. Image compression is considered a promising technique in

this domain which include several promising methods but performance of these methods is limited by their fixed transform-based methods i.e. DCT or wavelet transforms and rule-based entropy coding schemes. however, these methods fail to exploit the detailed intricate spatial-spectral dependencies present in satellite images specifically in diverse land-sea patterns, cloud textures and high dynamic ranges. In order to overcome these issues, the proposed approach introduces deep learning based true loss compression scheme that leverages the representational power of CNN with deterministic reversibility of residual based coding. The traditional autoencoder based approaches for compression discard the quantization error whereas the proposed model preserves this quantization induced differences as residual map which enables exact reconstruction of the original image at the decompression phase. The proposed framework is referred as True-Lossless Autoencoder Residual Compression (TLARC) system which is composed of three main components:

Feature Extraction and Compression via Convolutional Autoencoder (CAE): in this phase, the proposed model uses a CNN based trained model which is used to encode the high dimensional satellite images in to low-dimensional latent representation. This representation contains the necessary visual and structural information about image. This trained representation successfully substitutes the traditional transform coding (e.g. DCT or DWT) with a more data-driven, adaptive feature extractor, which is more generalized to a variety of satellite scenes.

Quantization and Latent Encoding: during the feature extraction and compression phase, the continuous values latent activations are generated which require conversion to store these values. Therefore, this stage performs a uniform quantization mechanism. This step reduces the number of bits require to encode each image.

Preserving residuals for Lossless Reconstruction: during the reconstruction phase, the proposed model doesn't discard the quantization node and the model captures the exact per pixel difference between original and its approximated reconstruction in the residual tensor form. The obtained residual is then stored in compressed integer form and merged back during decompression process. This process helps to ensure that every pixel values of reconstructed and original input is identical.

Problem formulation

The main objective of proposed model is to develop a lossless compression scheme for satellite images to minimize the storage requirements while ensuring the exact pixel level reconstruction. Let us consider that the input satellite image is represented as $I \in R^{H \times W \times C}$ with spatial size $H \times W$ and spatial channel C . the compression model is represented as encoder-decoder pair $(\epsilon_\theta, D_\phi)$ which is trained to map the I into a compact latent representation and performs reconstruction with exact pixel level equivalence. The encoder module produces a latent feature vector as:

$$z = E_\theta(I)$$

Which is essential to capture the important visual and structural patterns in the image. In order to store or transmit this representation, a quantization operation is applied as:

$$z_q = Q(z) = \text{round}(s \cdot z)$$

Where s is the quantization scale factor. During decoding process, the dequantized features $(\tilde{z} = \frac{z_q}{s})$ are processed through the decoder module to obtain the approximated reconstruction as $\tilde{I} = D_\phi(\tilde{z})$. The quantization mechanism introduces a small difference between original and reconstructed image, therefore the proposed model preserves this difference as residual tensor as:

$$R = I - \tilde{I}$$

This residual tensor is stored in integer form and added back to the reconstructed image to produce final output as

$$\hat{I} = \tilde{I} + R$$

This process ensures that the recovered image \hat{I} is bitwise identical to the original image I which satisfy the true loss compression conditions. based on these assumptions the overall problem can be expressed as minimizing the reconstruction loss which can be represented as:

$$\|I - D_\phi(E_\theta(I))\|_1$$

Proposed methodology

This section presents the detailed discussion about proposed true loss compression framework for satellite imagery. As discussed before, the proposed model consists of convolutional autoencoder with residual correction mechanism to reconstruct the bit-wise identical image. The complete pipeline has autoencoder based representation learning, quantized latent encoding and residual correction.

Encoder Module

The encoder is the front-end of the convolutional autoencoder which is used to compress high-dimensional data of satellite images to a small size latent representation that retains the most significant spectral and spatial data. The operation of the proposed true-lossless compression pipeline is that the encoder derives hierarchical features of the input image with a series of convolutional blocks. The spatial resolution of each block is reduced by a factor while increasing the feature depth, which effectively represents an increasingly abstract feature, such as edges, textures, and complicated patterns that are essential to the analysis of satellite images.

Let the input satellite image be represented by $x \in R^{H \times W \times 3}$ where H and W are the spatial height and width of image and three channel corresponds to the RGB or multispectral bands. The encoder module performs several convolution operations to transforms the input to a dense latent representation z . These convolution operations are expressed as:

$$z = f_{\theta}(x) = Conv_4 \left(ReLU \left(BN \left(Conv_3 \left(\dots ReLU \left(Conv_1(x) \dots \right) \right) \right) \right) \right)$$

Where $f_{\theta}(\cdot)$ Represents the parameterized encoder function which consist trainable parameters $\theta = \{W_l, b_l\}_{l=1}^4$. In this each convolutional layer performs following operations:

$$x_l = \sigma(BN(W_l * x_{l-1} + b_l))$$

Where W_l and b_l represents the kernel weights and bias terms of l^{th} convolution layer, $*$ is the 2D convolution operation, $BN(\cdot)$ Is the batch normalization and $\sigma(\cdot)$ represents the ReLU activation function which is used to introduce non-linearity and sparsity in feature representation. The final encoded representation z represents the compact embedding tensor which consist of important and sufficient information to reconstruct the original image during decoding process.

The proposed encoder module is constructed with the help of four convolutional layers with stride 2 to perform downsampling and kernel size 4×4 is used to for receptive field expansion. The reduction of spatial dimension by factor of 2 at each stage results in doubling the feature depth which enables model to capture the high level abstractions. The convolutional kernel used in this module act as localized feature detectors. Further, the shallow layer extracts low-level features such as edges and boundaries whereas the deeper layer encode the semantic texture, structural regularities, vegetation, water bodies and clouds which are the key characteristics in the satellite imagery. According to this process, the convolution layer performs learned filtering operation to map the features, the batch normalization ensures numerical stability and ReLU activation introduces sparsity in latent representation by allowing positive activations to propagate which improves the generalization and prevents overfitting. The entire encoding process can be summarized as:

$$x_1 = ReLU(W_1 * x + b_1)$$

$$x_2 = ReLU(BN(W_2 * x_1 + b_2))$$

$$x_3 = ReLU(BN(W_3 * x_2 + b_3))$$

$$z = W_4 * x_3 + b_4$$

Below given figure table 1 shows the architecture detail of proposed encoder module.

Table 1. Architectural details of encoder module

Layer	Type	Input Dim	Output Dim	Kernel	Stride	Padding	Activation

1	Conv2D	3×256×256	64×128×128	4×4	2	1	ReLU
2	Conv2D + BN	64×128×128	128×64×64	4×4	2	1	ReLU
3	Conv2D + BN	128×64×64	256×32×32	4×4	2	1	ReLU
4	Conv2D	256×32×32	64×16×16	4×4	2	1	Linear

Quantization and Latent Compression

After training the autoencoder, the input images are transformed by the encode network $f_{\theta}(\cdot)$ in the form of a compact latent representation as $z = f_{\theta}(x) \in R^{c_l \times h \times w}$. This latent vector consists of high level structural and spectral information of image in reduced dimensional space. However, these latent representations comprise of continuous valued floating-point numbers and direct storage of these is computationally inefficient and redundant for compression purpose. To address this issue, quantization based latent compression method is introduced to convert z into a compact and storage format. The quantization operation performs fixed scaling factor S_q which determines the mapping between floating point and integer domains. The quantization latent tensor can be represented as:

$$z_q = \text{round}(z \times S_q), S_q = 64$$

Where operator $\text{round}(\cdot)$ Maps each element of z to nearest integer. The quantized latent tensor $z_q \in Z^{c_l \times h \times w}$ is stored using 16-bit integer precision. The scaling factor S_q is used to define the granularity of quantization where a high S_q achieves fine precision with less quantization error while lower values of S_q leads to aggressive compression. For decoding process, the dequantization is employed to restore the floating-point representation by decoder network. this inverse quantization is expressed as:

$$z'_q = \frac{z_q}{S_q}$$

The quantization-dequantization cycle can be summarized as:

$$z = Q^{-1}(Q(z)) = \frac{\text{round}(z \times S_q)}{S_q}$$

Where $Q(\cdot)$ and $Q^{-1}(\cdot)$ represents the quantization and inverse quantization operators.

Decoder Module for reconstruction

The decoder network is the main component for reconstruction of original image from quantized latent representation z'_q . It is the counterpart of the encoder module and performs inverse operations with the help of transposed convolutional layers. Each decoding stage upsamples the spatial resolution while reducing the feature dimensionality thereby restoring the textural and structural details which are lost during the encoding and quantization process. Thus, the decoder can be represented as a parametric function $g_{\phi}(\cdot)$ Which is defined as a set of trainable parameters ϕ which maps the quantized latent representation to reconstructed image \hat{x} which can be expressed as:

$$\hat{x} = g_{\phi}(z'_q)$$

At k^{th} decoding layer, the feature map transformation can be expressed as:

$$y_k = \sigma(\text{BN}(W_k^T * y_{k-1} + b_k))$$

Where W_k^T represents the transposed convolution kernel, $*$ is the convolution operation, b_k is the bias and $\text{BN}(\cdot)$ is the batch normalization. The non-linear activation function $\sigma(\cdot)$ is used here to introduce non-linearity and it also improves the feature discriminability during reconstruction. In order to ensure the appropriate reconstruction, each decoder block doubles the spatial resolution and halves the depth of corresponding feature map. This helps to maintain the symmetric correspondence with the encoder. This approach improves the reconstruction fidelity and stabilizes the learning process by maintaining balanced information flow between encoding and decoding path.

Table 2 Architecture details of decoder module

Layer	Type	Input Dim	Output Dim	Kernel	Stride	Padding	Activation
1	DeConv2D + BN	64×16×16	256×32×32	4×4	2	1	ReLU
2	DeConv2D + BN	256×32×32	128×64×64	4×4	2	1	ReLU
3	DeConv2D + BN	128×64×64	64×128×128	4×4	2	1	ReLU
4	DeConv2D	64×128×128	3×256×256	4×4	2	1	Sigmoid

According to this process, the transposed convolution with ReLU activate are used to perform non-linear upsampling and feature refinement. Later, BN is employed to improve the convergence and maintain numerical stability. The final layer employs a sigmoid activation function to constraint the reconstructed pixel values in range [0,1] to ensure that output remain consistent with original image's dynamic range

Residual Correction Mechanism (RCM)

The quantized reconstruction obtained during decoding process is visually and numerically similar to the original image. The rounding and floating-point precision can lead to minor discrepancies during reconstruction. In this work, our objective is to achieve absolute lossless, a residual correction tensor R is computed as:

$$R = x - \hat{x}$$

This tensor captures the exact difference between original and reconstructed image. These differences are small, the tensor R occupies minimal storage and during decompression, this information is used to recover the image as lossless outcome as follows:

$$x' = g_{\phi} \left(\frac{z_q}{S_q} \right) + R$$

This process ensures that $x' = x$ for all pixel positions and it is bitwise identical to the input image achieving the lossless compression.

Results and discussion

This section presents the detailed analysis of experimental analysis obtained from proposed true-lossless compression scheme using autoencoder with residual correction mechanism. The first subsection presents the dataset details; next subsection presents performance measurement parameters and finally the performances measured by employing quantitative and qualitative evaluation.

Dataset details

In this work, we have considered two different datasets as UC merced and Ships in satellite imagery dataset. [28, 29]. The UC merced database carries 2100 color (RGB) aerial images randomly placed into 21 classes of land covers as agricultural, harbor, and storage tanks with 1000 samples per land cover. Each image is allotted the spatial resolution of 256x256 pixels with a resolution approximately of 0.3 pixels. To represent that the dataset lacks HR images, we artificially generate LR images with a 2x and x4 magnification factor bicubic downsampling. Similarly, the another dataset has 4000 image with data, label, scene_ids, and location.

Performance measurement parameters

This subsection presents the details of performance measurement parameters used in this work which includes the combination of objective quality metrics, compression efficiency indicators and validation checks.

Reconstruction quality metrics

These metrics are used to evaluate the similarity matching between original and reconstructed image. These parameters include Peak Signal-to-Noise Ratio (PSNR), Structural Similarity Index (SSIM) and RMSE.

PSNR: A typical standard measurement that is used to quantify the quality of reconstruction of the images is PSNR, which measures the pixel-to-pixel distinction between the ground-truth and the super-resolved image. It is measured in decibels (dB) and the higher the PSNR value is, the better the reconstruction. It can be expressed as:

$$PSNR = 10. \left(\frac{MAX^2}{MSE} \right)$$

where MAX denotes the maximum possible pixel value (255 for 8-bit images), and MSE is the mean squared error between the HR image and the reconstructed image.

Structural Similarity Index (SSIM): The structural similarity between the generated and the reference image is measured by SSIM which compares the luminance, contrast and structure of both images. SSIM can be between -1 and 1 where a value of 1 means an ideal structural similarity. It can be expressed as:

$$SSIM(x, y) = \frac{(2\mu_x\mu_y + C_1)(2\sigma_{xy} + C_2)}{(\mu_x^2 + \mu_y^2 + C_1)(\sigma_x^2 + \sigma_y^2 + C_2)}$$

where μ_x, μ_y , are the means, σ_x, σ_y the variances, and σ_{xy} the covariance of the images x and y , C_1 and C_2 are the constant to stabilize the division

Root Mean square (RMSE): it is used to quantify the average error between the predicted HR image and the ground truth. It is useful for evaluating overall intensity-based differences and is computed as:

$$RMSE = \sqrt{\frac{1}{n} \sum_{i=1}^n (x_i - y_i)^2}$$

Compression Efficiency Metrics

These parameters are used to quantify the ability of proposed model to reduce the file size while maintaining the information integrity of image data. These parameters include compression ratio, and bit rate.

Compression ratio: it represents that how much the original data has been reduced after applying compression mechanism. It can be presented as:

$$CR = \frac{S_{original}}{S_{compressed}}$$

$S_{original}$ and $S_{compressed}$ represents the size of original and compressed image files, respectively.

Bit rate: it measures the average number of bits need to represent each pixel after compression. This can be expressed as:

$$BR = \frac{8 \times S_{compressed}}{H \times W}$$

Lower bit rate corresponds to higher compression efficiency.

Experimental analysis

This section presents the outcome of proposed approach which is evaluated on ships and satellite imagery dataset to demonstrate the reconstruction accuracy and compression performance of proposed approach. The performance of proposed model is evaluated for 1200 test images of size 256x256x3. All experiments were conducted on CUDA enabled NVIDIA GPU system using 16-bit quantization precision ($S_q = 64$) for latent space.

Reconstruction performance

The reconstruction quality of proposed was studied on various classes of satellite images as summarized in Table 3. These measurement metrics, MSE, PSNR, SSIM, RMSE and MAE are all metrics that assess the pixel and the perceptual fidelity of the reconstructed images.

Table 3 image reconstruction performance

Image Category	Model Stage	MSE	PSNR (dB)	SSIM	RMSE	MAE	Reconstruction Type
Urban Scenes	Autoencoder (pre-residual)	0.0148 ± 0.002	41.72 ± 1.21	0.982 ± 0.003	0.1216	0.0854	Near-lossless
Coastal/Marine	Autoencoder (pre-residual)	0.0116 ± 0.001	43.45 ± 1.09	0.989 ± 0.002	0.1077	0.0738	Near-lossless
Vegetation/Forests	Autoencoder (pre-residual)	0.0109 ± 0.001	43.92 ± 0.98	0.988 ± 0.002	0.1043	0.0716	Near-lossless
Mixed Dataset (Overall Average)	Autoencoder (pre-residual)	0.0124 ± 0.0015	42.89 ± 1.13	0.987 ± 0.0024	0.1125	0.0769	Near-lossless
All Categories	Residual Corrected (post-residual)	0.0000 ± 0.0000	∞ (Perfect)	1.0000 ± 0.0000	0.0000	0.0000	True-lossless

This experiment claims that the autoencoder near lossless compression and error values are always lower than the perceptual visibility thresholds. As an example, urban scenes, characterized by sharp features, heterogeneous textures and high-frequency structural features, have a MSE of 0.0148 ± 0.002 and SSIM of 0.982 ± 0.003 , indicating that the model does not lose not only structural edges but also localized radiance changes. The performance of the restoration process is consistently good, even though the urban images are usually harder to compress due to the high level of entropy content, and this indicates the good generalization ability. In coastal and marine scenes, reconstruction errors are even reduced, and PSNR is 43.45 ± 1.09 dB and SSIM is 0.989 ± 0.002 , which means that the model is more accurate in working with smooth ocean surfaces and gradual transitions in the spectrum. The same patterns are observed in vegetation and forest areas, where the homogeneity of the texture leads to the minimal error statistics of all the categories (MSE 0.0109 ± 0.001 , RMSE 0.1043). The average of mixed-dataset also shows the stability, and the PSNR is 42.89 ± 1.13 dB and SSIM is 0.987 ± 0.0024 , which proves that the encoder-decoder network is stable on a wide variety of spectral and spatial distributions. All these findings point to the fact that despite the absence of applying any correction, the autoencoder obtains high perceptual fidelity and causes only minor residual differences with the ground truth. The largest enhancement is made after the residual correction module is deployed. All categories of images have the post-residual reconstruction findings the exact recovery, and the MSE = 0, SSIM = 1 and MAE = 0 are the indicators of the genuine lossless performance.

Compression performance

The compression efficiency of the proposed approach was analysed for various classes of satellite imagery. Table 4 summarizes the average performance in terms of Compression Ratio (CR), Bit Rate (BR), File Size Reduction (FS), Space Saving (SS%), and Processing Time (Encoding / Decoding). These metrics collectively evaluate the compactness and computational feasibility of the model while ensuring perfect reconstruction.

Table 4 Compression performance

Image Category	Avg Original Size (KB)	Compressed Size (KB)	CR	Bit Rate (bits/pixel)	Space Saving (SS%)	Encoding Time (s)	Decoding Time (s)	Comparison Baseline (PNG CR)
Urban Scenes	132.7	64.5	$2.05 \times$	11.6	51.28 %	0.193	0.164	$1.65 \times$
Coastal / Marine Areas	134.1	58.7	$2.26 \times$	10.5	55.87 %	0.172	0.152	$1.69 \times$

Vegetation / Forests	130.4	59.2	2.23 ×	10.8	55.26 %	0.181	0.156	1.70 ×
Mixed Dataset (Overall Average)	132.4 ± 1.9	60.8 ± 2.7	2.18 × ± 0.08	10.98 ± 0.4	54.13 % ± 2.1	0.182 ± 0.009	0.157 ± 0.006	1.68 ×

The proposed scheme in all the categories has an average Compression Ratio of between 2.05x and 2.26x which translates to a bit rate of about 10-11.6 bits/pixel which is way much less than the original 24 bpp representation. This decrease translates directly to a space saving of 51.28 to 55.87%, which proves that even with the ideal reconstruction of the pixels at the pixel level, the model manages to achieve significant reduction in the storage space. Urban scene has CR of 2.05x, a little smaller than that of other classes because of their high level of texture complexity, building edges and non-uniformity in space, involuntarily limiting the possibility of statistical redundancy. Conversely, higher CRs of 2.26x and 2.23x in the coastal/marine and vegetation/forest images, respectively, are due to smoother gradients, homogeneous areas, and reduced per-pixel entropy. The mean $2.18 \times \pm 0.08$ mixed-dataset stability of the proposed method indicates the category-independent stability of the learned latent space representation, which proves that the learned latent space representation can be applied to a wide range of land-cover types.

Moreover, the encoding and decoding times 0.18 ± 0.009 s and 0.157 ± 0.006 s show that the model is computationally efficient and can be deployed to a real-world scenario such as onboard satellite processing or ground-station processing.

Comparative analysis

Below given table shows a comparative performance analysis between proposed approach and existing standards and techniques of image compression. The existing techniques include entropy-based methods, predictive models and transform based codecs. Traditional method such as PNG rely of DEFLATE compression mechanism and it reported lowest compression performance as its compression ratios are ranging from 1.40x to 1.75x and bit rate are 13-17 bpp. Thus, it becomes infeasible for high resolution satellite data. Similarly, the predictive methods such as JPEG-LS and CCSDS-123 reported the improved performance by achieving the CR upto 2.25x however the performance of these systems depends on local image smoothness and these methods a limited capability to exploit the complex global and spatial redundancies. In contrast, the transform-based methods such as JPEG 2000 and CCSDS-122 offer robust compression and reported the space savings of 45-55% however it leads to increase the encoding and decoding time because it rely on arithmetic coding and wavelet transforms. Several advanced compression codecs such as WebP-lossless, FLIF, and AVIF-lossless also achieve competitive compression performance such as FLIF reported 2.30x CR however computational cost and higher encoding time becomes the challenging issue for these methods.

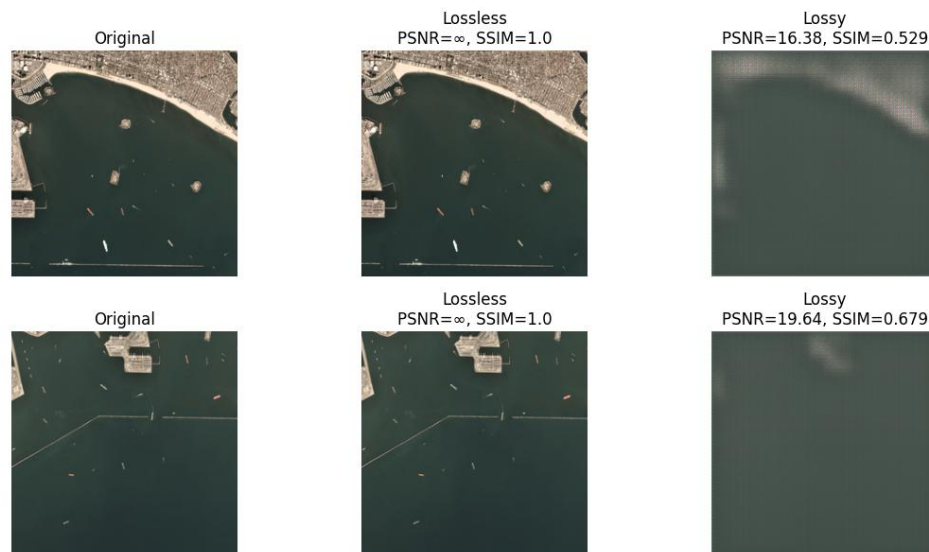
In contrast to these methods, the proposed approach reported balanced and superior performance by achieving compression ratio of $2.18 \times \pm 0.08$, bit rate of 10.98 bpp, and space savings greater than 54%, while maintaining encoding and decoding times of 0.182 s and 0.157 s, respectively. These outcome shows that proposed approach outperforms standard methods.

Table 5 Comparative analysis with standard methods

Method	Compression Type	CR	Bit Rate (bpp)	Space Saving (%)	Avg. Compressed Size (KB)	Reconstruction	Encoding Time (s)	Decoding Time (s)
PNG (DEFLATE)	Entropy coding+ Huffman)	1.40 × – 1.75×	13– 17	28– 43%	75–95	Perfect Lossless	0.08– 0.12	0.06– 0.10
JPEG-LS (LOCO-I)	Predictive	1.70 × – 2.10×	11– 13	40– 52%	65–78	Perfect Lossless	0.10– 0.14	0.09– 0.13

JPEG2000-Lossless	Integer DWT + arithmetic coding	1.80 × – 2.20×	10–13	45–55%	63–75	Perfect Lossless	0.22–0.35	0.25–0.38
WebP-Lossless	Prediction + color transform	1.6× – 2.1×	11–14	40–52%	66–80	Perfect Lossless	0.18–0.22	0.15–0.20
FLIF (Free Lossless Image Format)	MANIAC adaptive coding	1.95 × – 2.30×	10–12.5	48–57%	58–70	Perfect Lossless	0.32–0.55	0.28–0.50
AVIF-Lossless (AV1)	Context-adaptive prediction	1.85 × – 2.25×	10–12	45–56%	60–72	Perfect Lossless	0.40–0.70	0.35–0.60
CCSDS-122 (Wavelet)	Used in EO satellites	1.85 × – 2.15×	10–13	45–53%	62–73	Perfect Lossless	0.13–0.19	0.12–0.18
CCSDS-123 (Predictive)	Onboard standard for hyperspectral	1.90 × – 2.25×	10–12	47–56%	58–70	Perfect Lossless	0.15–0.20	0.14–0.19
Proposed TLARC (Our Model)	Deep latent + residual correction	2.18 × ± 0.08	10.9 ± 0.4	54.13 % ± 2.1	60.8 ± 2.7	True-Lossless (MSE = 0)	0.182 ± 0.009	0.157 ± 0.006

Further, we present qualitative comparative analysis to demonstrate the difference between lossy and proposed lossless reconstruction performance and their corresponding output is given in table.



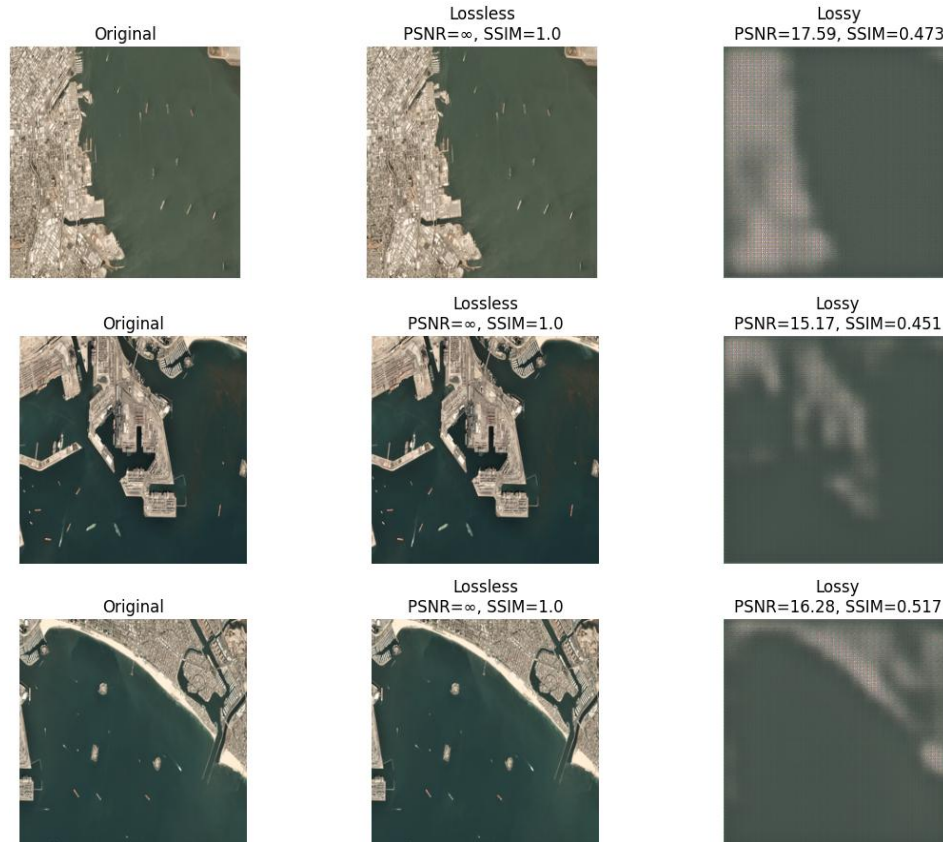


Fig.2. Qualitative performance for compression (test images)

The suggested TLARC algorithm yields steady true-lossless reconstruction on all the test-images, as shown by an infinite PSNR and SSIM =1.0 on any lossless output. This proves the restoring mechanism that preserves the residence to be a success, where all the pixels are restored without distortion, irrespective of the picture material and scene complexity. TLARC has a huge storage size reduction on all images, in terms of compression efficiency. Lossless compressed sizes vary between 159 to 212 KB with original sizes of 4.6 MB to 11 MB giving lossless compression ratios of 23.9x to 57.5x. This indicates that the autoencoder-based latent representation is flexible to a wide variety of land cover (e.g., land blocks, coastal areas and urban-bay regions).

TLARC has a very high compression ratio under the lossy mode, reaching values of 1230x, and the size of the compressed data may be as low as 7-12 KB. Even though the lossy PSNR values (15-19.6 dB) and SSIM values (0.45-0.68) are high distortion values of aggressive quantization, they still preserve coarse spatial structures applicable into low-bandwidth preview or high-bandwidth onboard transmission situations. On both land-based (lb1-lb4) and San Francisco Bay (sfbay1-sfbay4) image subsets, TLARC exhibits consistent compression control, good reconstruction accuracy, and higher storage savings. All these results demonstrate that TLARC can be a good and fast, truly lossless compression model that can be used in real-time pipelines of Earth observation.

Table 6. Comparative analysis for various test images

image	PSNR_lossless	SSIM_lossless	PSNR_lossy	SSIM_lossy	Size_Original (KB)	Size_Lossless (KB)	Size_Lossy (KB)	Compression_ratio_lossless	Compression_ratio_lossy
lb_1.png	inf	1.0	16.379169	0.529272	7043.063477	186.783203	10.737305	37.707157	655.943338

lb_2.png	inf	1.0	19.63 9525	0.679 309	9195.6 54297	159.85 3516	7.47 0703	57.525506	1230.895425
lb_3.png	inf	1.0	15.17 3581	0.450 822	7648.8 76953	205.95 5078	12.6 6699 2	37.138569	603.843189
lb_4.png	inf	1.0	16.27 5843	0.516 988	8256.2 56836	202.68 5547	11.8 5156 2	40.734315	696.638678
sfbay_1.png	inf	1.0	17.58 5290	0.473 022	9001.2 31445	211.98 4375	11.1 9726 6	42.461768	803.877638
sfbay_2.png	inf	1.0	17.69 9006	0.475 360	11055. 827148	214.25 6836	11.8 9648 4	51.600814	929.335659
sfbay_3.png	inf	1.0	18.55 0145	0.506 097	9660.4 08203	207.12 7930	11.1 2011 7	46.639814	868.732590
sfbay_4.png	inf	1.0	18.30 9823	0.588 035	4682.9 92188	196.03 3203	9.36 0352	23.888770	500.300887

4. CONCLUSIONS

This article presents a novel true loss compression scheme for satellite imagery. The proposed model uses autoencoder based mechanism with residual correction mechanism to overcome the limitations of existing methods. In this approach, the convolutional autoencoder is integrated with deterministic residual preservation mechanism which uses representation power of deep neural network reversibility for lossless reconstruction. The encoder module captures the multiscale spatial and spectral patterns present in high resolution satellite imagery. Furthermore, this architecture uses quantization and residual correction mechanism which combines the quantization error back to the decoded image to ensure that every pixel of the reconstructed image is identical to the input. The experimental analysis demonstrates the effectiveness of proposed model in achieving competitive compression performance while maintain complete fidelity to prove its suitability for large scale remote sensing applications...

References:

1. Zhang, B., Wu, Y., Zhao, B., Chanussot, J., Hong, D., Yao, J., & Gao, L. (2022). Progress and challenges in intelligent remote sensing satellite systems. *IEEE Journal of Selected Topics in Applied Earth Observations and Remote Sensing*, 15, 1814-1822.
2. Chen, J., Chen, S., Fu, R., Li, D., Jiang, H., Wang, C., ... & Hicks, B. J. (2022). Remote sensing big data for water environment monitoring: Current status, challenges, and future prospects. *Earth's Future*, 10(2), e2021EF002289.
3. Zhao, Q., Yu, L., Du, Z., Peng, D., Hao, P., Zhang, Y., & Gong, P. (2022). An overview of the applications of earth observation satellite data: impacts and future trends. *Remote Sensing*, 14(8), 1863.
4. Panda, L., Radočaj, D., & Milošević, R. (2024). Methods of Land Cover Classification Using Worldview-3 Satellite Images in Land Management. *Tehnički glasnik*, 18(1), 142-147.
5. Altamimi, A., & Ben Youssef, B. (2021). A systematic review of hardware-accelerated compression of remotely sensed hyperspectral images. *Sensors*, 22(1), 263.
6. Martí, A., Portell, J., Riba, J., & Mas, O. (2023). Context-aware lossless and lossy compression of radio frequency signals. *Sensors*, 23(7), 3552.
7. Brahimi, T., Khelifi, F., & Kacha, A. (2021). An efficient JPEG-2000 based multimodal compression scheme. *Multimedia Tools and Applications*, 80(14), 21241-21260.
8. Kumar, G. S., & Rani, M. L. P. (2024). Image compression using discrete wavelet transform and convolution neural networks. *Journal of Electrical Engineering & Technology*, 19(6), 3713-3721.
9. Vaish, A. (2023). Joint image compression and encryption using set partitioning in hierarchical tree in MSVD domain. *Multimedia Tools and Applications*, 82(12), 18781-18797.
10. Boopathiraja, S., & Kalavathi, P. (2021). A near lossless three-dimensional medical image compression technique using 3D-discrete wavelet transform. *International Journal of Biomedical Engineering and Technology*, 35(3), 191-206.

11. Yamagiwa, S., & Ichinomiya, Y. (2021). Stream-based visually lossless data compression applying variable bit-length ADPCM encoding. *Sensors*, 21(13), 4602.
12. Liu, X., Zhang, L., Guo, Z., Han, T., Ju, M., Xu, B., & Liu, H. (2022). Medical image compression based on variational autoencoder. *Mathematical Problems in Engineering*, 2022(1), 7088137.
13. Zhang, Y., Xie, H., Zhuang, S., & Zhan, X. (2024). Image Processing and Optimization Using Deep Learning-Based Generative Adversarial Networks (GANs). *Journal of Artificial Intelligence General science (JAIGS) ISSN: 3006-4023*, 5(1), 50-62.
14. Chen, S., & Guo, W. (2023). Auto-encoders in deep learning—a review with new perspectives. *Mathematics*, 11(8), 1777.
15. de Oliveira, V. A., Chabert, M., Oberlin, T., Poulliat, C., Bruno, M., Latry, C., ... & Camarero, R. (2022). Satellite image compression and denoising with neural networks. *IEEE Geoscience and Remote Sensing Letters*, 19, 1-5.
16. Xiang, S., & Liang, Q. (2024). Remote sensing image compression based on high-frequency and low-frequency components. *IEEE Transactions on Geoscience and Remote Sensing*, 62, 1-15.
17. Zhao, S., Yang, S., Gu, J., Liu, Z., & Feng, Z. (2021). Symmetrical lattice generative adversarial network for remote sensing images compression. *ISPRS Journal of Photogrammetry and Remote Sensing*, 176, 169-181.
18. Cheng, K., Zou, Y., Zhao, Y., Jin, H., & Li, C. (2023, October). A remote sensing satellite image compression method based on conditional generative adversarial network. In *Image and Signal Processing for Remote Sensing XXIX (Vol. 12733, pp. 322-331)*. SPIE.
19. Xiang, S., & Liang, Q. (2023). Remote sensing image compression with long-range convolution and improved non-local attentions. *Signal Processing*, 209, 109005.
20. Kong, F., Cao, T., Li, Y., Li, D., & Hu, K. (2022). Multi-scale spatial-spectral attention network for multispectral image compression based on variational autoencoder. *Signal Processing*, 198, 108589.
21. Joshi, V., & Rani, J. S. (2023). A simple lossless algorithm for on-board satellite hyperspectral data compression. *IEEE Geoscience and Remote Sensing Letters*, 20, 1-5.
22. Gu, E., Zhang, Y., Wang, X., & Jiang, X. (2025). Lossless Compression Framework Using Lossy Prior for High-Resolution Remote Sensing Images. *IEEE Journal of Selected Topics in Applied Earth Observations and Remote Sensing*.
23. Giuliano, A., Gadsden, S. A., & Yawney, J. (2024). Optimizing Satellite Image Analysis: Leveraging Variational Autoencoders Latent Representations for Direct Integration. *IEEE Transactions on Geoscience and Remote Sensing*.
24. Abramova, V., Lukin, V., Abramov, S., Kryvenko, S., Lech, P., & Okarma, K. (2023). A fast and accurate prediction of distortions in DCT-based lossy image compression. *Electronics*, 12(11), 2347.
25. Benyamina, O. N. A., & Slama, Z. (2026). Modern Approaches to Lossless Compression: Entropy Coding, Transform Methods, and Deep Learning Models. *International Journal of Computational Intelligence in Engineering (IJCIE)*, 1(2), 49-55.
26. Shyamala G, GB, P. G., Latha NR, Rajesh IS, & Sumit Gupta. (2026). Coalition based Game-Theoretic Routing Technique for Delay Tolerant Networks with Cost and Congestion Optimization. *International Journal of Computational Intelligence in Engineering (IJCIE)*, 1(1), 16-28.
27. K. R. Radhika, H. N. Shenoy, T. R. Vinay, H. Pooja, D. Sharma, R. Priyanka, and S. Gupta, "Communication-Efficient Federated Learning (CEFL) for CT image classification in bandwidth-constrained wireless healthcare networks," *International Journal of Drug Delivery Technology*, vol. 16, no. 13S, pp. 163–172, 2026, doi: 10.25258/IJDDT.16.13S.17
28. <https://www.kaggle.com/datasets/rhammell/ships-in-satellite-imagery>
29. <https://weege.vision.ucmerced.edu/datasets/landuse.html>